Published OnlineFirst March 8, 2016; DOI: 10.1158/1078-0432.CCR-15-2903

Biology of Human Tumors

Clinical Cancer Research

Transposon Mutagenesis Reveals Fludarabine Resistance Mechanisms in Chronic Lymphocytic Leukemia

Tatjana Pandzic[1], Jimmy Larsson[1], Liqun He[1], Snehangshu Kundu[1], Kenneth Ban[1,2], Muhammad Akhtar-Ali[1], Anders R. Hellström[1], Anna Schuh[3], Ruth Clifford[3], Stuart J. Blakemore[4], Jonathan C. Strefford[4], Tycho Baumann[4], Armando Lopez-Guillermo[5], Elias Campo[6], Viktor Ljungström[1], Larry Mansouri[1], Richard Rosenquist[1], Tobias Sjöblom[1], and Mats Hellström[1]

Abstract

Purpose: To identify resistance mechanisms for the chemotherapeutic drug fludarabine in chronic lymphocytic leukemia (CLL), as innate and acquired resistance to fludarabine-based chemotherapy represents a major challenge for long-term disease control.

Experimental Design: We used *piggyBac* transposon-mediated mutagenesis, combined with next-generation sequencing, to identify genes that confer resistance to fludarabine in a human CLL cell line.

Results: In total, this screen identified 782 genes with transposon integrations in fludarabine-resistant pools of cells. One of the identified genes is a known resistance mediator *DCK* (deoxycytidine kinase), which encodes an enzyme that is essential for the phosphorylation of the prodrug to the active metabolite. *BMP2K*, a gene not previously linked to CLL, was also identified as a modulator of response to fludarabine. In addition, 10 of 782 transposon-targeted genes had previously been implicated in treatment resistance based on somatic mutations seen in patients refractory to fludarabine-based therapy. Functional characterization of these genes supported a significant role for *ARID5B* and *BRAF* in fludarabine sensitivity. Finally, pathway analysis of transposon-targeted genes and RNA-seq profiling of fludarabine-resistant cells suggested deregulated MAPK signaling as involved in mediating drug resistance in CLL.

Conclusions: To our knowledge, this is the first forward genetic screen for chemotherapy resistance in CLL. The screen pinpointed novel genes and pathways involved in fludarabine resistance along with previously known resistance mechanisms. Transposon screens can therefore aid interpretation of cancer genome sequencing data in the identification of genes modifying sensitivity to chemotherapy. *Clin Cancer Res; 22(24); 6217–27. ©2016 AACR.*

Introduction

Chronic lymphocytic leukemia (CLL) is a clinically and biologically heterogeneous disease. Although most patients are asymptomatic at diagnosis and only a minor proportion of patients will experience rapid disease progression and early treatment, the majority of patients will develop a more aggressive disease requiring therapy over the coming years (1). To identify patients with an expected inferior outcome, detection of certain recurrent cytogenetic aberrations (i.e., deletion of 11q, 13q, and 17p, and trisomy 12) and *TP53* mutational screening is currently recommended for all patients before initiation of therapy (1–3). In fact, *TP53* aberrations, that is, del(17p) and/or *TP53* mutations, are associated with a particularly short time to progression, poor response to therapy, and the worst overall survival of all subtypes of CLL (1).

The gold standard first-line chemoimmunotherapy for medically fit CLL patients is a combination treatment, that is, fludarabine, cyclophosphamide, and the anti-CD20 antibody rituximab (FCR), with overall response rates of 90% to 95% (4, 5). However, most patients will eventually relapse and 10% of patients are also primary fludarabine refractory (FR). Approximately 40% of the primary FR patients have somatic *TP53* mutations, further underscoring the key role of p53 in drug response (6, 7). ATM dysfunction, because of del(11q) and *ATM* mutations, is also associated with reduced response to FC, but, in contrast to *TP53* aberrations, patients with del (11q) have an improved response rate with the addition of rituximab (4, 8).

[1]Department of Immunology, Genetics and Pathology, Science for Life laboratory, Uppsala University, Uppsala, Sweden. [2]Department of Biochemistry, Yong Loo Lin School of Medicine, NUS, Institute of Molecular and Cell Biology, A*STAR, Singapore. [3]Radcliffe Department of Medicine, Oxford University, Oxford, United Kingdom. [4]Cancer Sciences, Faculty of Medicine, University of Southampton, Southampton, United Kingdom. [5]Servicio de Hematología, Hospital Clínic, IDIBAPS, Barcelona, Spain. [6]Unitat de Hematología, Hospital Clínic, IDIBAPS, Universitat de Barcelona, Barcelona, Spain.

Note: Supplementary data for this article are available at Clinical Cancer Research Online (http://clincancerres.aacrjournals.org/).

T. Pandzic and J. Larsson contributed equally to this article.

Current address for J. Larsson: Department of Cell and Molecular Biology, Uppsala University, Uppsala, Sweden.

Corresponding Author: Mats Hellström, Uppsala University, Dag Hammarskjöldsv. 20, Uppsala 75185, Sweden. Phone: 461-8471-4002; Fax: 461-855-8931; E-mail: mats.hellstrom@igp.uu.se

doi: 10.1158/1078-0432.CCR-15-2903

Published OnlineFirst March 8, 2016; DOI: 10.1158/1078-0432.CCR-15-2903

Translational Relevance

We performed a *piggyBac* transposon mutagenesis screen in a human CLL cell line to identify genes and pathways involved in fludarabine resistance. This screen revealed both known and novel genes mediating drug resistance, in contrast to previous transposon screens that only identified already known genes. Three new candidate genes for drug resistance to fludarabine were identified, that is, *BMP2K*, *ARID5B*, and *BRAF*, and a key role for the MAPK pathway was implicated. Hence, the study provides a proof-of-principle that transposon mutagenesis can generate important functional data regarding drug response, thus complementing ongoing large-scale mutational analyses in clinical materials.

The recent development of next-generation sequencing (NGS) technologies has been successful in identifying not only genes driving CLL ontogeny and evolution, but also in revealing mutations that are predictive for therapy response (reviewed in ref. 9). So far, mutations in *SF3B1*, *BIRC3*, *NOTCH1*, *POT1*, *FAT1*, *SAMD1*, and *IKZF3*, have been identified as enriched in patients relapsing after FCR or with FR disease (10–17). Regardless of this, there is still a significant fraction of CLL patients relapsing after FCR, where the genetic cause of resistance remains elusive. Similar to other cancer types, NGS efforts in CLL require large patient cohorts and longitudinally collected samples to pinpoint new genetic alterations as causally involved in drug resistance and formal proof also requires experimental validation. Therefore, alternative approaches complementing the existing sequencing efforts in patients could greatly improve the interpretation of NGS data.

In this study, we performed a *piggyBac* transposon mutagenesis screen, which is the first forward genetic screen to identify genes modifying drug response in CLL. *piggyBac* transposon mutagenesis has been applied to identify mechanisms of chemotherapy resistance to purine analogues (6-thioguanine) and taxanes (paclitaxel), while also aiding the identification of novel second site mutations in *BRAF* in response to vemurafenib (18–20). Our analysis revealed both novel genes, not previously implicated in chemotherapy resistance in CLL, as well as genes already linked to refractory disease thus validating our approach.

Materials and Methods

Cell culture

The human EBV-transformed, lymphoblastoid cell line HG3, established from a poor prognostic CLL patient with unmutated IGHV genes (further characterized in ref. 21) was propagated in RPMI1640 medium supplemented with 0.5 × Glutamax, 10% heat-inactivated FBS, and 1% PEST (all from Gibco/Life Technologies). The human colorectal cancer cell lines RKO, its isogenic derivative RKO $BRAF^{wt/-/-}$ (both from Horizon Discovery), and HCT116 (ATCC) were maintained in McCoy 5A medium supplemented with 10% FBS and 1% PEST (all from Gibco/Life Technologies). HCT116 $TP53^{-/-}$ and its parental HCT116 $TP53^{+/+}$ cell line (kindly provided by B. Vogelstein, Johns Hopkins University, Baltimore, MD) were cultured in DMEM (Gibco/Life Technologies) supplemented with 10% FBS and 1% PEST.

piggyBac transposon screen

Transposon and transposase (HyPBase) constructs are schematically illustrated in Supplementary Fig. S1. A total of 15–30 × 10^6 HG3 cells were coelectroporated with 3 μg of the transposase and transposon plasmids using the Amaxa Nucleofector Kit R (Lonza) with the program W-01. Following a 48-hour recovery, the cells were grown either under selection with 3 μmol/L F-ara-A (Sigma Aldrich), the nucleoside prodrug of fludarabine, or no selection for 6 to 12 weeks. During this time, the cells were passaged twice per week and each time seeded at a density of 100,000 cells/mL in a t75 culture flask. Following this, F-ara-A–resistant cells were treated with 250 μg/mL hygromycin B (Life Technologies) to select only those cells with active transposon insertions. The treatment continued until no viable cells remained in a control HG3 cell culture (not transfected with transposon/transposase).

Cell viability assay

Following hygromycin selection of cells with transposon insertions, cell pools that were either treated or untreated with F-ara-A were tested for F-ara-A sensitivity using a resazurin viability assay. Briefly, 100,000 cells were seeded in 1 mL in triplicate wells in a 24-well plate and treated with increasing concentrations of F-ara-A (ranging from 1 to 64 μmol/L) for 72 hours. To assess growth suppression, 44 μmol/L resazurin (Sigma Aldrich) was added to the medium and fluorescence was measured in a Wallac Victor Multilabel Counter (Wallac) with excitation and emission wavelengths of 530 and 590 nm, respectively. The relative number of viable cells was expressed as percentage of untreated cells.

Splinkerette PCR

Genomic DNA was isolated from cell pools with the NucleoSpin DNA Extraction Kit (Machery Nagel). Splinkerette PCR was performed as described previously (22). Briefly, following digestion of genomic DNA with Sau3AI, DNA was ligated to adaptors and a primary PCR reaction was performed with a Splink1- 5′-CGAAGAGTAACCGTTGCTAGGAGAGACC-3′ and HMsp1-5′-CGAAGAGTAACCGTTGCTAGGAGAGACC-3′ primer pair (20). Secondary PCR was carried out with barcoded primers (Supplementary Material and Methods) and the products were treated with ExoSap. The barcoded samples were mixed in equimolar concentrations and sequenced on an Illumina HiSeq 2000 instrument.

Sequence processing and identification of genes with transposon integrations

To map the transposon integrations, the sequences were trimmed to remove the barcode and adaptor sequences, then aligned to human genome (hg19) using the Smalt software (www.sanger.ac.uk/resources/software/smalt, version 0.7.5.1, with default parameters). The mapped sequences were parsed to identify the genomic integration locations, together with the number of the sequences that support the integrations. To identify candidate genes with a significant number of integration sites, the observed and expected integrations for each Ensembl gene were computed (23) and Poisson statistics were used to calculate a *P* value for each gene. To correct for multiple hypothesis testing, the false discovery rates were calculated for each candidate gene. Detailed description of data analysis is shown in Supplementary Material and Methods.

Published OnlineFirst March 8, 2016; DOI: 10.1158/1078-0432.CCR-15-2903

Transfection, plasmids, and shRNA vectors

The pGIPZ lentiviral shRNA vectors targeting DCK (RHS4430-20031599, RHS4430-200183211, RHS4430-200189164), BMP2K (RHS4430-200166293, RHS4430-200234236, RHS4430-200237243), UBR5 (RHS4430-200269761, RHS4430-200215630), and a nonsilencing pGIPZ control vector (RHS4346) were purchased from Thermo Scientific. HG3 cells were electroporated with 5 μg of each vector using the Amaxa Nucleofector Kit R (Lonza) with the program W-01. Pools of HG3 cells stably expressing indicated shRNAs were selected in 1 μg/mL puromycin for 6 to 8 weeks.

For gene overexpression analyses, a Myc-tagged ARID5B construct was purchased from Origene (RC211454), whereas the Flag-tagged LARS was from Addgene (plasmid 46341, D. Sabatini; PMID: 23723238). DCK and NUDCD3 ORFeome clones [ORFeome Collaboration (OC) cDNA Clones: http://www.orfeomecollaboration.org] were obtained from the core facility Karolinska High Throughput Center http://www.scilifelab.se/facilities/khtc and subsequently cloned into a Vivid Colors pcDNA6.2/C-EmGFP-DEST Mammalian Expression Vector (Life Technologies). The empty pcDNA3 vector was used as a control. Transfection of HCT116 cells was performed with Lipofectamine 2000 (Life Technologies) using 5 μg of recombinant construct.

To assess the sensitivity to F-ara-A following transient or stable transfection, cells were seeded in either 96-well plates (HCT116 and RKO; 8,000 cells/well) or 24-well plates (HG3; 100,000 cells/well) and treated with increasing concentrations of the drug (ranging from 2 to 128 μmol/L for HCT116 and RKO cells and from 1 to 64 μmol/L for HG3 cells) for 72 hours. The growth suppression was evaluated using a viability assay as described.

Western blot analysis

Cells were lysed in NP40 buffer in the presence of protease inhibitors (Complete Mini; Roche) and phosphatase inhibitors (Halt Phosphatase Inhibitor Cocktail; Thermo Scientific). An aliquot of 50 μg total protein was run on an SDS-PAGE gel and transferred to a nitrocellulose membrane (GE Healthcare). Primary antibodies used were anti-Myc (Cell Signaling Technology; 1:1,000), anti-pERK1/2 (Cell Signaling Technology; #4377, 1:1,000), anti-ERK1/2 (Cell Signaling Technology; #4696, 1:1,000), anti-α-tubulin (T8203, Sigma Aldrich; 1:1,000), anti-Flag (Sigma Aldrich F3165, 1:1,000), and anti-β-actin (Abcam ab6276, 1:2,000). Immunoreactive proteins were visualized with SuperSignal West Femto Chemiluminescent Substrate (Thermo Scientific) on the ImageQuant LAS 4000 imaging system (GE Healthcare).

Real-time quantitative PCR

Total RNA was extracted using an RNeasy Plus Mini Kit (Qiagen) and cDNA was synthesized using a Maxima H Minus First Strand cDNA Synthesis Kit (Thermo Scientific). Real-time quantitative PCR was performed with Maxima SYBR Green/Rox qPCR Master Mix (Thermo Scientific) in a StepOne qPCR instrument (Applied Biosystems; primers are listed in Supplementary Materials and Methods). Data were analyzed by employing the $\Delta\Delta C_t$ method with the software provided by Applied Biosystems Inc., using *ACTB* as the reference gene.

RNA sequencing

RNA samples were prepared as described. The RNA integrity and concentration was determined on a Bioanalyzer instrument (Agilent) using an RNA 6000 Nano Kit. Samples were sequenced on the Ion Proton system (Ion Torrent/Life Technologies. In each sample, approximately 30 to 50 million reads were sequenced. The reads were aligned to the human genome hg19 assembly (https://genome.ucsc.edu) using Tophat2 software (version 2.0.4; ref. 24). The RNAseq read count quantification was performed using the HTSeq tool (version 0.6.1; ref. 25). To identify the gene expression differences between the three pairs of HG3 pools, DESeq2 software was used (26).

BRAF screening of CLL patient samples

Using whole-exome/genome sequencing, the mutation status of *BRAF* was assessed in 506 Spanish patients as recently reported (15). In addition, samples from 247 untreated patients enrolled in the UK LRF CLL4 clinical trial (27) were investigated using targeted NGS including the *BRAF* gene.

Statistical analysis

GraphPad Prism 6.0b was used for statistical analysis. Dose–response data were analyzed using nonlinear regression and log (inhibitor) versus response—variable slope (four parameters) to calculate IC_{50} values from viability tests. Statistical significance was calculated using Student *t* test for IC_{50} values for specific doses of F-ara-A. All data shown are based on at least three independent experiments. For the Spanish cohort, time-to-first-treatment (TTFT) was measured from time of sampling until date of first treatment, and overall survival (OS) from time of sampling until the last follow-up or death. For the UK LRF CLL4 trial patients, OS was calculated from randomization date until the last follow-up or death, whereas progression-free survival (PFS) was measured from randomization until event. Survival curves were constructed using the Kaplan–Meier method and the log-rank test was applied to determine differences between survival proportions using the Statistica Software 12.0 (Stat Soft Inc.).

Results

A forward genetic screen to identify fludarabine resistance genes in CLL

Three independent pools of the transposon mutagenized human CLL cell line (HG3) were generated and selected in 3 μmol/L of F-ara-A (the nucleoside pro-drug of fludarabine) for 6 to 12 weeks (Fig. 1 and Supplementary Fig. S1). Each HG3 pool was estimated to contain 2–4 $\times$ 10^5 independent insertions after transfection, which corresponds to the potential activation of 95% of the genome (18). After selection in F-ara-A, each pool exhibited two- to 5-fold reduced sensitivity to F-ara-A, as compared with parental HG3 (Fig. 1 and Supplementary Fig. S1B and S1C). No difference in F-ara-A sensitivity was seen in mutagenized HG3 cells that were not cultured in F-ara-A or in nonmutagenized HG3 cells that were cultured in F-ara-A (Fig. 1 and Supplementary Fig. S1, and data not shown). Splinkerette PCR was applied to amplify the flanking regions of the transposon insertions and high-throughput sequencing of the PCR products were performed to identify the location of the transposons (Fig. 1).

Published OnlineFirst March 8, 2016; DOI: 10.1158/1078-0432.CCR-15-2903

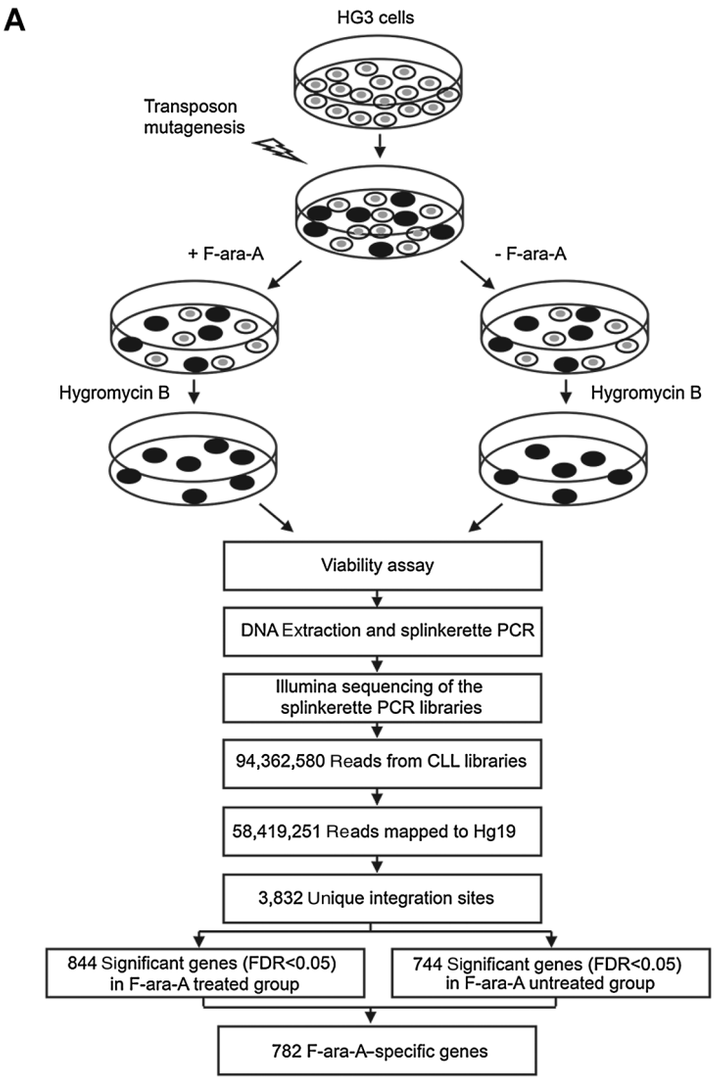

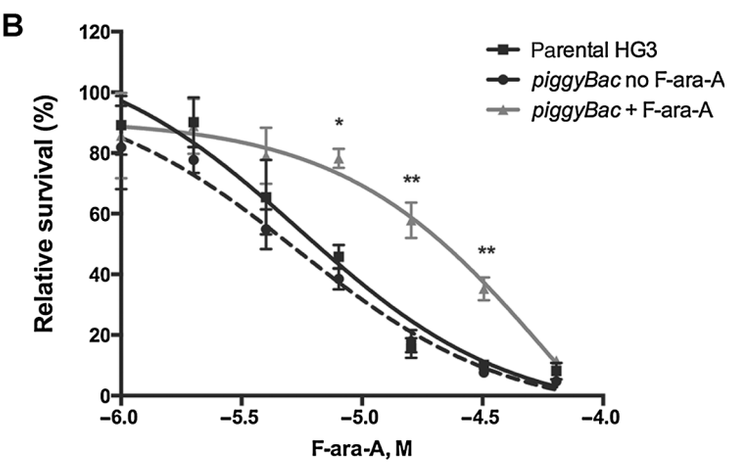

Figure 1.
A *piggyBac* transposon-based screen generates pools of HG3 cells with reduced sensitivity to fludarabine. **A,** HG3 cells (white and gray circles) were electroporated (lightning) with *piggyBac* transposon and transposase (Supplementary Fig. S1) and subsequently selected in the presence of 3 μmol/L (+F-ara-A) or absence of fludarabine (−F-ara-A). Cells were passaged twice weekly and cultured for 6 to 12 weeks and thereafter selected in Hygromycin B to allow survival of only the transposon-containing HG3 cells (black circles). This removed cells that had potentially become resistant to F-ara-A by means other than transposon insertion. Subsequent cell viability tests with increasing concentrations of F-ara-A revealed resistant pools of HG3 cells. Cell pools were harvested for DNA and RNA extraction and processed for splinkerette PCR to identify insertion sites for *piggyBac* transposon. **B,** Titration of F-ara-A showing a pool of *piggyBac* mutagenized HG3 cells with 3-fold reduced sensitivity to fludarabine. Parental HG3 (black line, IC_{50}: 6.4 μmol/L, a pool of HG3 cells that had been mutagenized with *piggyBac* and selected in F-ara-A (*piggybac* + F-ara-A) IC_{50}: 20.9 μmol/L and a pool of HG3 cells that had been mutagenized with *piggyBac* but not selected in F-ara-A (*piggybac* - F-ara-A) IC_{50}: 6.2 μmol/L). The individual doses with statistically significant differences are indicated with stars (*, $P < 0.05$; **, $P < 0.01$), the error bars indicate SEM.

Published OnlineFirst March 8, 2016; DOI: 10.1158/1078-0432.CCR-15-2903

Table 1. The top ranking genes mediating resistance to fludarabine identified in the *piggyBac* screen

Gene (HGNC symbol)	Description	TTAA sites	Expected insertions	Observed insertions	Cell pool	*P* value	*P* value FDR
SNX5	Sorting nexin 5	235	0.02	8	17. 28	0	0
MGME1	Mitochondrial genome maintenance exonuclease 1	172	0.02	8	17. 28	0	0
EIF2AK3	Eukaryotic translation initiation factor 2-alpha kinase 3	634	0.04	6	17. 28	6.86E−14	1.57E−11
DCK	Deoxycytidine kinase	348	0.03	4	17	4.24E−10	3.88E−08
SLC1A3	Solute carrier family 1 (glial high affinity glutamate transporter), member 3	609	0.04	4	17	1.43E−09	1.19E−07
RBM34	RNA binding motif protein 34	184	0.02	3	17	6.68E−09	5.11E−07
TRIM31	Tripartite motif containing 31	76	0.01	2	28	4.00E−08	2.62E−06
NUDT8	Nudix (nucleoside diphosphate linked moiety X)-type motif 8	5	0.00	1	28	1.00E−07	6.11E−06
BMP2K	BMP2 inducible kinase	1415	0.14	4	28	4.31E−07	1.96E−05
MOB1A	MOB kinase activator 1A	201	0.014	2	28	4.71E−07	1.96E−05

NOTE: The ranking was based on frequency of observed transposon integrations in relation to number of total potential *piggyBac* insertion sites (4 nt recognition site, TTAA) within the genes and 5 kb upstream of the genes. Only protein encoding genes expressed in HG3 cells, according to the RNA-sequencing data (normalized FPKM value greater than 0.1), were considered as plausible candidates. The *P* values were calculated using Poisson statistics, with false discovery rate (FDR) correction for multiple tests and a corrected *P* value < 0.05 as cutoff for selection of significant genes.
Abbreviation: HGNC, HUGO Gene Nomenclature Committee.

Validation of genes mediating fludarabine resistance

Collectively, this screen identified 782 genes with transposon integrations not overlapping with genes identified in the nonselected pools (Supplementary Table S1). Among the top 10 most significantly targeted genes by the transposon insertions was deoxycytidine kinase (*DCK*), which encodes an essential step in the activation of the purine nucleoside analogue fludarabine, where it phosphorylates the nucleoside (F-ara-A) to nucleoside-monophosphate (Table 1). This indicates that the screen indeed can identify genes modifying fludarabine sensitivity. While performing splinkerette PCR, a single strong band was observed on the gel in addition to the expected smear. This band was isolated and Sanger sequenced and identified as an insertion within *BMP2K*, one of the top 10 transposon targeted genes out of the 782 identified (Table 1). We next performed shRNA-mediated knock-downs of *BMP2K* and *DCK*, which led to a robust down-regulation of the *BMP2K* and *DCK* transcripts (Supplementary Fig. S2) and protein (data not shown). Titration of F-Ara-A resulted in a 2.5- and 3.3-fold increase in IC_{50} when *BMP2K* and *DCK* had been knocked-down as compared with HG3 cells expressing control shRNA (Fig. 2A).

To identify potentially clinically relevant mechanisms for acquired resistance to F-ara-A, the gene sets identified by *piggyBac* transposon mutagenesis were intersected with 148 genes found somatically mutated in CLL patients refractory to fludarabine-based therapy (12). Overall, 10 genes were found in common between the transposon and the genomic screen, which is a significant enrichment compared to the expected enrichment occurring by chance (hypergeometric probability $P = 0.034$; Table 2). *ARID5B*, *BRAF*, *LARS*, *NUDCD3*, and *UBR5* were selected for functional validation, primarily based on their gene expression in CLL and in the HG3 cell line. The choice of validation using cDNA overexpression or shRNA-mediated knock-down was based on transposon insertion, where *piggyBac* insertion upstream or in first or second intron in a sense orientation suggested an activation event that was validated by gene overexpression. In contrast, *piggyBac* insertion within the gene and in an antisense orientation indicated gene silencing.

shRNA-mediated knock-down of *UBR5* led to robust down-regulation of the mRNA, but did not result in any alteration in the IC_{50} value for F-ara-A (data not shown). Because of the poor transfection efficiency of HG3 cells, we decided to use adherent cell lines to allow for overexpression of plasmids as well as the use of available isogenic cell lines. To test the validity of the colorectal cancer cell line HCT116, we titrated F-ara-A in parental and *TP53* knockout cells. In agreement with the known role of p53 in response to fludarabine-based treatment, HCT116 *TP53* knockout cells showed a three-fold reduced sensitivity for F-ara-A, suggesting that HCT116 cells recapitulate some key features of fludarabine response and resistance (Supplementary Fig. S3). Transfection of GFP-tagged expression vectors in HCT116 cells resulted in approximately 20% to 30% of the cells being GFP-positive (Supplementary Fig. S4). As predicted, transient transfection of *DCK* resulted in an increased sensitivity to F-ara-A, with IC_{50} of 30 μmol/L for DCK-expressing cells versus 35 μmol/L for control cells (Fig. 2B). Given the low frequency of cells expressing the plasmids, it is still a significant and sizable change. Overexpression of *ARID5B* resulted in a modest but significant increase in F-ara-A IC_{50}, 41 μmol/L for ARID5B-expressing cells versus 35 μmol/L for control cells (*t* test; $P = 0.0064$), whereas no difference was observed between *LARS*- or *NUDCD3*-expressing and control HCT116 cells (Fig. 2C and data not shown).

The case of BRAF

A transposon insertion was identified in the first intron of the serine/threonine kinase *BRAF*, which is compatible with gene activation (Fig. 2E). Noteworthy, an activating L597Q *BRAF* mutation was recently identified in one patient reported to be refractory to fludarabine-based therapy (12). To test whether *BRAF* activation confers a reduced sensitivity to fludarabine, we used the colorectal RKO cell line that harbors the activating V600E mutation in *BRAF* and its isogenic derivative where the mutant alleles have been knocked out. The presence of V600E was associated with significantly reduced sensitivity to higher doses of F-ara-A, as revealed by cell viability assay (Fig. 2D). The difference in response to F-ara-A between *BRAF*-mutant and

Published OnlineFirst March 8, 2016; DOI: 10.1158/1078-0432.CCR-15-2903

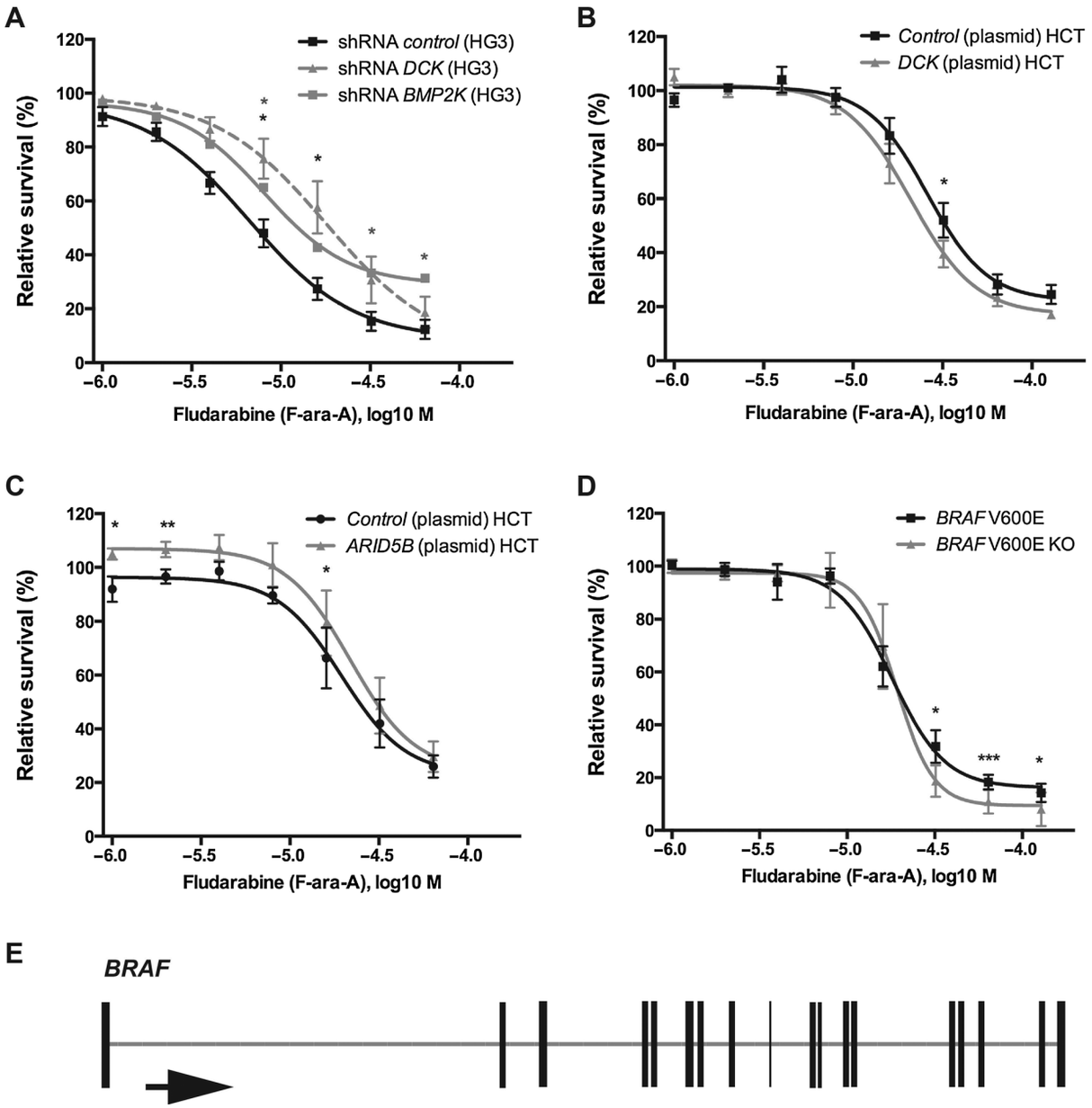

Figure 2.

The putative fludarabine resistance genes *DCK, BMP2K, ARID5B*, and *BRAF* confer acquired resistance to fludarabine. **A,** Summary of F-ara-A dose–response curves of HG3 cells expressing control shRNA (black line and boxes) or shRNA targeting *DCK* (gray line and triangles) and *BMP2K* (gray dashed line and boxes). Knockdown of either gene confers reduced sensitivity to F-ara-A as compared to control cells. **B,** Summary of dose–response curves from HCT116 cells of overexpression of *DCK* (gray line and triangles) resulted in an increase in sensitivity to F-ara-A as compared to control vector (black line and boxes). **C,** Overexpression of *ARID5B* (gray line and triangles) in HCT116 cells led to reduced sensitivity to F-ara-A as compared to control vector (black line and boxes). **D,** Summary of dose–response experiments of F-ara-A in human RKO colorectal cancer cells (*BRAF* V600E, black line and boxes) and an isogenic derivative where the mutant *BRAF* allele had been knocked out (*BRAF* V600E KO, gray line and triangles). *BRAF* V600E confers reduced sensitivity to F-ara-A. The individual doses with statistically significant differences are indicated with black asterisks or grey asterisks in A for shRNA *DCK* (HG3) (*, $P < 0.05$; **, $P < 0.01$; ***, $P < 0.001$); the error bars indicate SEM. **E,** Schematic representation of the transposon integration within the intron 1 of the *BRAF* gene. Transposon element is shown as a black arrow, where the direction of the arrow indicates orientation of integration.

wild-type cells was normalized by the addition of the BRAF V600E inhibitor vemurafinib (Supplementary Fig. S5).

To investigate the significance of *BRAF* mutations in CLL patients, we analyzed whole-exome/genome data available from a "general practice" cohort. Ten of 506 patients carried nonsynonymous *BRAF* mutations (median variant allele frequency, 36%, range, 17–58%). Notably, patients with *BRAF* mutation had a significantly shorter TTFT compared to wild type (median 0.5 vs. 64.5 months, $P < 0.001$), whereas no significant difference was seen for OS (median 128.0 months vs. 122.9 months,

Published OnlineFirst March 8, 2016; DOI: 10.1158/1078-0432.CCR-15-2903

Table 2. Genes overlapping between *piggyBac* mutagenesis and genes found somatically mutated in CLL patients refractory to fludarabine-based therapy

Gene (HGNC symbol)	Mutation (Messina *et al.*)	Location	Strand	Expression in CLL[a]	Expression in HG3[b]
ACSS3	L305V	Upstream	−	Low	Present
ANO2	F614fs	Intron 7	+	Low	Absent
ARID5B	N297T	Upstream, intron 1	+	High	Present
BRAF	L597Q	Intron 1	+	Moderate	Present
CCDC80	D872E	Intron 2	−	Low	Absent
LARS	I852V	Intron 1	−	Moderate to high	Present
NUDCD3	H144Y	Intron 2	+	Moderate	Present
PDE7B	E350K	Intron 2	−	Low	Absent
TMEM132B	A911S	Intron 1, intron 4	+	Low	Present
UBR5	A2154V	Intron 1	−	High	Present

NOTE: The mutation identified by Messina and colleagues is presented as an amino acid location in the protein. Location refers to the transposon insertion in relation to the targeted gene. Strand, + indicates the same direction of the *piggyBac* cassette and gene transcription; − indicates the opposite direction of the *piggyBac* cassette relative to gene transcription. Genes shown in bold were selected for functional validation.

Abbreviation: HGNC, HUGO Gene Nomenclature Committee.

[a]Based on Genesapiens; low: <300; moderate: 300–1,000; high: > 1,000.

[b]Based on RNA sequencing data in HG3 cells. Transcripts with a normalized fragment per kilobase of transcript per million fragments mapped (FPKM) value less than 0.1 were considered "absent."

$P = 0.98$; Fig. 3; Supplementary Table S2). Nine of 10 *BRAF*-mutant patients required treatment within 2 years. We also investigated 247 cases from the UK CLL4 trial and detected eight patients with *BRAF* mutations (median variant allele frequency, 32%, range, 12–50%; Supplementary Table S2); however, no significant difference in OS or PFS was observed (OS 79.0 months vs. 75.0 months, $P = 0.97$; PFS 39.0 months vs. 24.0 months, $P = 0.53$).

The MAPK signaling pathway and fludarabine resistance in CLL

Pathway analysis of the 782 genes identified in the transposon screen using gene-set enrichment analysis (GSEA; refs. 28, 29) showed an enrichment of genes in cancer-related pathways and MAPK signaling (Table 3). In fact, one third of the genes in the cancer-related pathways belonged to the MAPK pathway (Supplementary Table S3).

To address whether the fludarabine-resistant HG3 cells were transcriptionally different at a global level compared with their parental cells, we performed RNA sequencing of three pairs of HG3 pools. This analysis revealed 302 genes that were significantly differentially expressed (more than 2-fold) and hierarchical clustering demonstrated distinct and stable changes in the RNA expression patterns in the fludarabine-resistant HG3 pools versus the parental cell lines (Supplementary Fig. S6; Table S4). Comparing the mRNA expression profiles of the HG3-resistant pools to reported profiles using GSEA ("oncogenic signatures") revealed significant similarities to 35 other mRNA expression signatures (Supplementary Table S5). Nine were related to MAPK signaling, due to the activation of *EGFR*, *KRAS*, *CRAF*, *MEK1*, or inactivation of *STK33*.

Taken together, the experimental validation of *BRAF*, the bioinformatics analysis of transposon insertions, and the transcriptional deregulation of the MAPK pathway indicate a role for the MAPK pathway in fludarabine resistance. In line with this, phosphorylated ERK was also increased in a fludarabine-refractory HG3 pool (Supplementary Fig. S7).

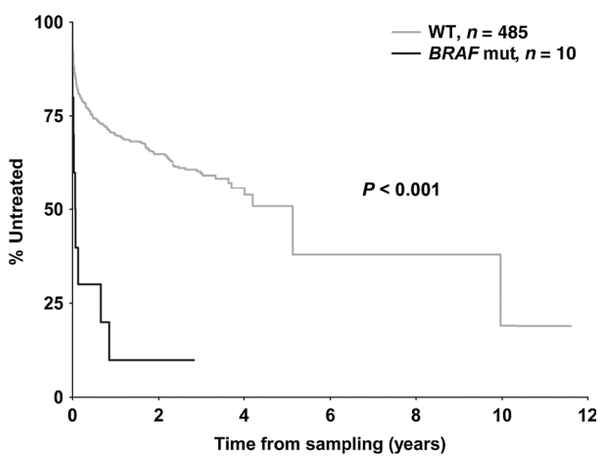

Figure 3.
Time to first treatment in CLL patients with and without *BRAF* mutation. *BRAF*-mutant patients exhibit significantly shorter time to first treatment compared with *BRAF* wild-type patients (log-rank test, $P < 0.001$). Median time from diagnosis to sampling in BRAF-mutated cases was 0.65 years (0–3.46 years).

Discussion

Interpretation of data from large-scale cancer genome sequencing studies is often hampered by the high frequency of passenger mutations, sequencing artifacts, and small cohort sizes. Complementary approaches are therefore needed to assign relevant functions to genes identified as mutated in cancer to understand the genetics and biology driving cancer development and to provide insights into mechanisms of resistance to therapy. *piggyBac* transposon mutagenesis is a powerful forward genetics tool that can facilitate the identification of genes mediating resistance to chemotherapy. This technique has been successfully applied in transgenic mice and in cell culture systems for the discovery of genes driving cancer development and drug resistance (18–20, 30, 31).

To determine genetic mediators of resistance to fludarabine, we performed a *piggyBac* transposon screen in the HG3 CLL cell line and identified 782 transposon-targeted genes in pools of cells exhibiting fludarabine resistance. The identification of *DCK*, a known determinant of cellular response to fludarabine, underscores that the screen has the power to detect biologically relevant genes. DCK encodes a rate-limiting kinase in the activation of the prodrug F-ara-A to the nucleoside-monophosphate. Low levels of

Published OnlineFirst March 8, 2016; DOI: 10.1158/1078-0432.CCR-15-2903

Table 3. Top 10 Kyoto Encyclopedia of Genes and Genomes (KEGG) pathways identified by gene set enrichment analysis (GSEA)

Gene set name	No. of genes in gene set (K)	Description	No. of genes in overlap (k)	% of MAPK genes	FDR *q* value
KEGG PATHWAYS IN CANCER	328	Pathways in cancer	25	28 (7/25)	4.63E−9
KEGG NON SMALL CELL LUNG CANCER	54	Non–small cell lung cancer	9	44 (4/9)	7.68E−6
KEGG SMALL CELL LUNG CANCER	84	Small cell lung cancer	10	20 (2/10)	2.6E−5
KEGG ENDOCYTOSIS	183	Endocytosis	14	14 (2/4)	2.66E−5
KEGG UBIQUITIN MEDIATED PROTEOLYSIS	138	Ubiquitin mediated proteolysis	12	8 (1/12)	3.51E−5
KEGG MAPK SIGNALING PATHWAY	267	MAPK signaling pathway	16	100 (16/16)	7.34E−5
KEGG GLIOMA	65	Glioma	8	38 (3/8)	1.25E−4
KEGG MELANOMA	71	Melanoma	8	38 (3/8)	2.14E−4
KEGG ADHERENS JUNCTION	75	Adherens junction	8	0	2.86E−4
KEGG SNARE INTERACTIONS IN VESICULAR TRANSPORT	38	SNARE interactions in vesicular transport	6	0	3.21E−4

NOTE: K, number of genes in the pathway; k, number of genes overlapping with the KEGG pathway. The fraction of genes overlapping with MAPK pathway was based on the genes identified and is presented in Supplementary Table S2. Statistical significance is given as false discovery rate (FDR) *q* value with $q < 0.05$ used as cutoff for selection of significant pathways.

DCK have been shown to correlate with impaired response to fludarabine in CLL (32). In addition, reduced levels of DCK were also observed in mantle cell lymphoma patients exhibiting refractoriness to cytarabine, a member of the same class of drugs as fludarabine (33).

The *piggyBac* screen also identified *BMP2K* as a novel gene conferring resistance to fludarabine. *BMP2K* was first identified as a BMP2 inducible kinase that plays a role in osteoblast differentiation (34) and, together with BMP2, it was also shown to regulate eye development (35). The role of BMP signaling in B-cell malignancies is less clear, but it was reported that BMP6 inhibits the growth of mature B cells and that epigenetic inactivation of BMP6 was associated with more aggressive disease in diffuse large cell B-cell lymphomas (36, 37). Because BMP receptors are found upregulated in CLL cells, but not in normal B cells, it is plausible that BMP2K might act as an essential downstream target of BMP signaling in CLL (38). The fact that *BMP2K* was the only transposon-targeted gene in our screen that was detected by traditional Sanger sequencing following splinkerette PCR, indicates a possible enrichment of cell clones with this integration within the pool of fludarabine-resistant cells. Until now, *BMP2K* has not been linked to either CLL pathophysiology or the cellular response to fludarabine and elucidation of its role in these processes hence warrants further investigation.

To identify genes that could mediate fludarabine resistance of potential direct relevance to CLL patients, we compared the gene set identified in pools of *piggyBac*-mutagenized HG3 cells after selection in fludarabine with genes identified in a set of patients with FC-refractory CLL (12). The combined approach efficiently narrowed down the number of candidate genes from hundreds to 10 and their contribution to fludarabine resistance was functionally assessed *in vitro* using gene overexpression or gene knockdown approach. *ARID5B* was one of the genes identified and validated in the intersection between the *piggyBac* screen and genes found mutated in a FC-refractory patient. *ARID5B* is a member of the AT-rich interaction domain containing protein (ARID) family. This family consists of DNA-binding proteins that promote transcription via association with the SWI/SNF chromatin-remodeling complex (39). Interestingly, genome-wide association studies have revealed an association of a variant allele of *ARID5B* with an increased risk for childhood B-cell ALL and treatment outcome in ALL (40, 41). *ARID5B* is mutated in 6% to 23% of endometrial carcinoma, and *Arid5b* knockout mice exhibit defects in normal B-cell development (39, 42). In addition, the homolog *ARID1A* is a driver mutation in 1.6% of CLL patients and was also found mutated in splenic marginal zone lymphoma and germinal center–derived lymphomas (15, 43, 44). Thus, *ARID5B* is a plausible novel candidate for affecting CLL progression and response to treatment.

Another gene that was common to both the *piggyBac* screen and the analysis of patients with FC-refractory CLL was *BRAF*, where our validation experiments using cancer cell lines with an activating V600E mutation in *BRAF* confirmed that its activation may lead to fludarabine resistance. *BRAF* mutations have been recurrently reported in CLL patients with a frequency of approximately 3% (12, 14, 15, 45, 46). Although the most prevalent *BRAF* mutation in cancer in general is V600E, which leads to a constitutive activation of BRAF, mutations other than V600E are more frequently seen in CLL without any obvious hot-spot (Supplementary Fig. S8; Supplementary Table S6). However, most of them cluster within or near the activation loop where V600E resides and are known to confer variable, but increased signaling and oncogenic capacity (47). Given that most of the mutations may lead to increased BRAF activity, we speculate that the *BRAF* mutations observed in the activation loop in CLL patients act in a similar way with regards to fludarabine sensitivity, even though we cannot rule out that mutations other than V600E might behave differently. Of note, activating mutations in other members of the MAPK pathway have also been reported in CLL, for example, NRAS, KRAS, MAPK1 (ERK2), and ERG2 (14, 15, 45). Hence, if one considers the entire MAPK pathway it is possible that its contribution to CLL pathobiology is larger than previously thought (45, 46).

Transcriptional profiling of the fludarabine-refractory HG3 pools revealed distinct changes in mRNA expression that were similar to established "oncogenic" signatures observed after activation of EGFR, KRAS, CRAF, and MEK1. Three genes that were common to both fludarabine-resistant HG3 cells and activated *EGFR/KRAS/CRAF/MEK1* pathways had previously been linked to B-cell signaling and function, for example, *IGFBP4*, *PTPRE*, and *VAV3*. IGF4BP is an insulin growth factor (IGF) binding protein that modulates cell growth via IGF. It is upregulated in CLL and acts downstream of oncogenic KRAS and EGR1 (48, 49). PTPRE is a phosphatase expressed in leukocytes that is induced by antigen stimulation and regulates MAPK signaling (50). VAV proteins are critical for T- and B-cell receptor–induced Ca^{2+} signaling and NF-κB–mediated survival signaling in B cells (51, 52). In line with our findings from the

Published OnlineFirst March 8, 2016; DOI: 10.1158/1078-0432.CCR-15-2903

piggyBac screen, other studies have also suggested that RAF/MEK/ERK signaling has prosurvival effects under fludarabine treatment (53–55).

CLL cells are dependent on stromal cell interaction to prevent apoptosis and this protective effect is partially because of CXCL12–CXCR4 interaction that leads to induction of pERK and STAT3 and protects the CLL cells from fludarabine-induced apoptosis (53). In addition, inhibition of BRAF or MEK1 was shown to abrogate the protective effect of stromal cells (54), whereas cladribine, another purine nucleoside analogue, induces ERK phosphorylation and together with inhibition of MEK protein kinase acting upstream of ERK led to synergistic cell killing (55).

In our screening of CLL patient samples, the mutation status of *BRAF* was associated with shorter TTFT in the "general practice" cohort, whereas no difference was observed for OS. In line with the latter finding, investigation of patients requiring treatment from the UK CLL4 trial did not show any difference in PFS and OS. Hence, further studies on larger number of cases are imperative to determine the potential prognostic/predictive role of *BRAF* mutations in CLL.

Given the known importance of *TP53*, *ATM*, and *SF3B1* in clinical response to fludarabine-based therapy, it might at first appear surprising that these genes were not identified in this screen. However, considering the biologic heterogeneity of the disease, one CLL cell line (HG3), although established from a CLL patient with aggressive disease, may not capture all types of resistance patterns, and further investigation of additional CLL cell lines will be necessary to get different model systems representative of major CLL subtypes.

In conclusion, to our knowledge, this is the first forward genetic screen for genes mediating fludarabine resistance in an experimental system. Our data supports the notion that the combination of genetic screens in experimental systems and NGS-based mutational analyses of human samples complement each other in an efficient way to identify functionally relevant genes not only for CLL but also for other cancer types. In particular, we identified both known and novel mediators of fludarabine resistance, hence underscoring the broad applicability of this method and highlighting activation of BRAF/MAPK signaling and downstream targets as a central mechanism behind reduced fludarabine sensitivity in CLL.

Disclosure of Potential Conflicts of Interest

A. Schuh reports receiving speakers bureau honoraria from Abbvie, Gilead, Janssen, Novartis, Pharmacyclics, and Roche. J.C. Strefford reports receiving commercial research grants from Roche. No potential conflicts of interest were disclosed by the other authors.

Authors' Contributions

Conception and design: J. Larsson, M. Akhtar-Ali, T. Sjöblom, M. Hellström
Development of methodology: T. Pandzic, J. Larsson, L. He, S. Kundu, K. Ban, M. Akhtar-Ali, A.R. Hellström, M. Hellström
Acquisition of data (provided animals, acquired and managed patients, provided facilities, etc.): T. Pandzic, J. Larsson, M. Akhtar-Ali, A. Schuh, R. Clifford, S.J. Blakemore, J.C. Strefford, T. Bauman, A. Lopez-Guillermo, E. Campo, L. Mansouri, R. Rosenquist
Analysis and interpretation of data (e.g., statistical analysis, biostatistics, computational analysis): T. Pandzic, J. Larsson, L. He, K. Ban, M. Akhtar-Ali, R. Clifford, J.C. Strefford, T. Bauman, V. Ljungström, M. Hellström
Writing, review, and/or revision of the manuscript: T. Pandzic, J. Larsson, L. He, S. Kundu, M. Akhtar-Ali, A. Schuh, J.C. Strefford, E. Campo, V. Ljungström, L. Mansouri, R. Rosenquist, T. Sjöblom, M. Hellström
Administrative, technical, or material support (i.e., reporting or organizing data, constructing databases): A.R. Hellström, R. Rosenquist, M. Hellström
Study supervision: J.C. Strefford, M. Hellström

Grant Support

This research project was supported by the Swedish Cancer Society, the Swedish Research Council, The Beijer Foundation, the Lion's Cancer Research Foundation, and Selander's Foundation. Sequencing was performed by the SNP&SEQ Technology Platform, Science for Life Laboratory at Uppsala University, a national infrastructure supported by the Swedish Research Council (VRRFI) and the Knut and Alice Wallenberg Foundation. The computations were performed on resources provided by SNIC through Uppsala Multidisciplinary Center for Advanced Computational Science (UPPMAX) under Project b2014071. J.C. Strefford is supported by the Bloodwise (11052, 12036, 14027), the Kay Kendall Leukaemia Fund (873), and the Bournemouth Leukaemia Fund, with infrastructure support from a Cancer Research-UK Center grant (C34999/A18087).

The costs of publication of this article were defrayed in part by the payment of page charges. This article must therefore be hereby marked *advertisement* in accordance with 18 U.S.C. Section 1734 solely to indicate this fact.

Received November 27, 2015; revised February 16, 2016; accepted February 17, 2016; published OnlineFirst March 8, 2016.

References

1. Hallek M, Cheson BD, Catovsky D, Caligaris-Cappio F, Dighiero G, Dohner H, et al. Guidelines for the diagnosis and treatment of chronic lymphocytic leukemia: a report from the International Workshop on Chronic Lymphocytic Leukemia updating the National Cancer Institute-Working Group 1996 guidelines. Blood 2008;111:5446–56.
2. Dohner H, Stilgenbauer S, Benner A, Leupolt E, Krober A, Bullinger L, et al. Genomic aberrations and survival in chronic lymphocytic leukemia. N Engl J Med 2000;343:1910–6.
3. Pospisilova S, Gonzalez D, Malcikova J, Trbusek M, Rossi D, Kater AP, et al. ERIC recommendations on TP53 mutation analysis in chronic lymphocytic leukemia. Leukemia 2012;26:1458–61.
4. Hallek M, Fischer K, Fingerle-Rowson G, Fink AM, Busch R, Mayer J, et al. Addition of rituximab to fludarabine and cyclophosphamide in patients with chronic lymphocytic leukaemia: a randomised, open-label, phase 3 trial. Lancet 2010;376:1164–74.
5. Wierda W, O'Brien S, Wen S, Faderl S, Garcia-Manero G, Thomas D, et al. Chemoimmunotherapy with fludarabine, cyclophosphamide, and rituximab for relapsed and refractory chronic lymphocytic leukemia. J Clin Oncol 2005;23:4070–8.
6. Zenz T, Habe S, Denzel T, Mohr J, Winkler D, Buhler A, et al. Detailed analysis of p53 pathway defects in fludarabine-refractory chronic lymphocytic leukemia (CLL): dissecting the contribution of 17p deletion, TP53 mutation, p53-p21 dysfunction, and miR34a in a prospective clinical trial. Blood 2009;114:2589–97.
7. Zenz T, Eichhorst B, Busch R, Denzel T, Habe S, Winkler D, et al. TP53 mutation and survival in chronic lymphocytic leukemia. J Clin Oncol 2010;28:4473–9.
8. Stilgenbauer S, Schnaiter A, Paschka P, Zenz T, Rossi M, Dohner K, et al. Gene mutations and treatment outcome in chronic lymphocytic leukemia: results from the CLL8 trial. Blood 2014;123:3247–54.
9. Sutton LA, Rosenquist R. Deciphering the molecular landscape in chronic lymphocytic leukemia: time frame of disease evolution. Haematologica 2015;100:7–16.
10. Rossi D, Fangazio M, Rasi S, Vaisitti T, Monti S, Cresta S, et al. Disruption of BIRC3 associates with fludarabine chemorefractoriness in TP53 wild-type chronic lymphocytic leukemia. Blood 2012;119:2854–62.
11. Rossi D, Bruscaggin A, Spina V, Rasi S, Khiabanian H, Messina M, et al. Mutations of the SF3B1 splicing factor in chronic lymphocytic leukemia:

Published OnlineFirst March 8, 2016; DOI: 10.1158/1078-0432.CCR-15-2903

association with progression and fludarabine-refractoriness. Blood 2011; 118:6904–8.
12. Messina M, Del Giudice I, Khiabanian H, Rossi D, Chiaretti S, Rasi S, et al. Genetic lesions associated with chronic lymphocytic leukemia chemorefractoriness. Blood 2014;123:2378–88.
13. Landau DA, Carter SL, Stojanov P, McKenna A, Stevenson K, Lawrence MS, et al. Evolution and impact of subclonal mutations in chronic lymphocytic leukemia. Cell 2013;152:714–26.
14. Landau DA, Tausch E, Taylor-Weiner AN, Stewart C, Reiter JG, Bahlo J, et al. Mutations driving CLL and their evolution in progression and relapse. Nature 2015;526:525–30.
15. Puente XS, Bea S, Valdes-Mas R, Villamor N, Gutierrez-Abril J, Martin-Subero JI, et al. Non-coding recurrent mutations in chronic lymphocytic leukaemia. Nature 2015;526:519–24.
16. Quesada V, Conde L, Villamor N, Ordonez GR, Jares P, Bassaganyas L, et al. Exome sequencing identifies recurrent mutations of the splicing factor SF3B1 gene in chronic lymphocytic leukemia. Nat Genet 2012; 44:47–52.
17. Wang L, Lawrence MS, Wan Y, Stojanov P, Sougnez C, Stevenson K, et al. SF3B1 and other novel cancer genes in chronic lymphocytic leukemia. N Engl J Med 2011;365:2497–506.
18. Chen L, Stuart L, Ohsumi TK, Burgess S, Varshney GK, Dastur A, et al. Transposon activation mutagenesis as a screening tool for identifying resistance to cancer therapeutics. BMC Cancer 2013;13:93.
19. Choi J, Landrette SF, Wang T, Evans P, Bacchiocchi A, Bjornson R, et al. Identification of PLX4032-resistance mechanisms and implications for novel RAF inhibitors. Pigment Cell Melanoma Res 2014;27:253–62.
20. Wang W, Bradley A, Huang Y. A piggyBac transposon-based genome-wide library of insertionally mutated Blm-deficient murine ES cells. Genome Res 2009;19:667–73.
21. Rosen A, Bergh AC, Gogok P, Evaldsson C, Myhrinder AL, Hellqvist E, et al. Lymphoblastoid cell line with B1 cell characteristics established from a chronic lymphocytic leukemia clone by in vitro EBV infection. Oncoimmunology 2012;1:18–27.
22. Uren AG, Mikkers H, Kool J, van der Weyden L, Lund AH, Wilson CH, et al. A high-throughput splinkerette-PCR method for the isolation and sequencing of retroviral insertion sites. Nat Protoc 2009;4:789–98.
23. Brett BT, Berquam-Vrieze KE, Nannapaneni K, Huang J, Scheetz TE, Dupuy AJ. Novel molecular and computational methods improve the accuracy of insertion site analysis in Sleeping Beauty-induced tumors. PLoS One 2011;6:e24668.
24. Kim D, Pertea G, Trapnell C, Pimentel H, Kelley R, Salzberg SL. TopHat2: accurate alignment of transcriptomes in the presence of insertions, deletions and gene fusions. Genome Biol 2013;14:R36.
25. Anders S, Pyl PT, Huber W. HTSeq—a Python framework to work with high-throughput sequencing data. Bioinformatics 2015;31:166–9.
26. Love MI, Huber W, Anders S. Moderated estimation of fold change and dispersion for RNA-seq data with DESeq2. Genome Biol 2014;15:550.
27. Catovsky D, Richards S, Matutes E, Oscier D, Dyer MJ, Bezares RF, et al. Assessment of fludarabine plus cyclophosphamide for patients with chronic lymphocytic leukaemia (the LRF CLL4 Trial): a randomised controlled trial. Lancet 2007;370:230–9.
28. Mootha VK, Lindgren CM, Eriksson KF, Subramanian A, Sihag S, Lehar J, et al. PGC-1alpha-responsive genes involved in oxidative phosphorylation are coordinately downregulated in human diabetes. Nat Genet 2003; 34:267–73.
29. Subramanian A, Tamayo P, Mootha VK, Mukherjee S, Ebert BL, Gillette MA, et al. Gene set enrichment analysis: a knowledge-based approach for interpreting genome-wide expression profiles. Proc Natl Acad Sci U S A 2005;102:15545–50.
30. Mann MB, Black MA, Jones DJ, Ward JM, Yew CC, Newberg JY, et al. Transposon mutagenesis identifies genetic drivers of Braf melanoma. Nat Genet 2015;47:486–95.
31. Moriarity BS, Largaespada DA. Sleeping Beauty transposon insertional mutagenesis based mouse models for cancer gene discovery. Curr Opin Genet Dev 2015;30:66–72.
32. Mackey JR, Galmarini CM, Graham KA, Joy AA, Delmer A, Dabbagh L, et al. Quantitative analysis of nucleoside transporter and metabolism gene expression in chronic lymphocytic leukemia (CLL): identification of fludarabine-sensitive and -insensitive populations. Blood 2005;105: 767–74.
33. Klanova M, Lorkova L, Vit O, Maswabi B, Molinsky J, Pospisilova J, et al. Downregulation of deoxycytidine kinase in cytarabine-resistant mantle cell lymphoma cells confers cross-resistance to nucleoside analogs gemcitabine, fludarabine and cladribine, but not to other classes of anti-lymphoma agents. Mol Cancer 2014;13:159.
34. Kearns AE, Donohue MM, Sanyal B, Demay MB. Cloning and characterization of a novel protein kinase that impairs osteoblast differentiation *in vitro*. J Biol Chem 2001;276:42213–8.
35. Liu HP, Lin YJ, Lin WY, Wan L, Sheu JJ, Lin HJ, et al. A novel genetic variant of BMP2K contributes to high myopia. J Clin Lab Anal 2009; 23:362–7.
36. Daibata M, Nemoto Y, Bandobashi K, Kotani N, Kuroda M, Tsuchiya M, et al. Promoter hypermethylation of the bone morphogenetic protein-6 gene in malignant lymphoma. Clin Cancer Res 2007;13: 3528–35.
37. Kersten C, Sivertsen EA, Hystad ME, Forfang L, Smeland EB, Myklebust JH. BMP-6 inhibits growth of mature human B cells; induction of Smad phosphorylation and upregulation of Id1. BMC Immunol 2005;6:9.
38. Dzietczenia J, Wrobel T, Jazwiec B, Mazur G, Butrym A, Poreba R, et al. Expression of bone morphogenetic proteins (BMPs) receptors in patients with B-cell chronic lymphocytic leukemia (B-CLL). Int J Lab Hematol 2010;32(6 Pt 1):e217–21.
39. Lahoud MH, Ristevski S, Venter DJ, Jermiin LS, Bertoncello I, Zavarsek S, et al. Gene targeting of Desrt, a novel ARID class DNA-binding protein, causes growth retardation and abnormal development of reproductive organs. Genome Res 2001;11:1327–34.
40. Mullighan CG. Genetic variation and the risk of acute lymphoblastic leukemia. Leukemia Res 2010;34:1269–70.
41. Xu H, Cheng C, Devidas M, Pei D, Fan Y, Yang W, et al. ARID5B genetic polymorphisms contribute to racial disparities in the incidence and treatment outcome of childhood acute lymphoblastic leukemia. J Clin Oncol 2012;30:751–7.
42. The Cancer Genome Atlas Research Network, Kandoth C, Schultz N, Cherniack AD, Akbani R, Liu Y, et al. Integrated genomic characterization of endometrial carcinoma. Nature 2013;497:67–73.
43. Lunning MA, Green MR. Mutation of chromatin modifiers; an emerging hallmark of germinal center B-cell lymphomas. Blood Cancer J 2015;5: e361.
44. Parry M, Rose-Zerilli MJ, Ljungstrom V, Gibson J, Wang J, Walewska R, et al. Genetics and prognostication in splenic marginal zone lymphoma: revelations from deep sequencing. Clin Cancer Res 2015;21:4174–83.
45. Damm F, Mylonas E, Cosson A, Yoshida K, Della Valle V, Mouly E, et al. Acquired initiating mutations in early hematopoietic cells of CLL patients. Cancer Discov 2014;4:1088–101.
46. Jebaraj BM, Kienle D, Buhler A, Winkler D, Dohner H, Stilgenbauer S, et al. BRAF mutations in chronic lymphocytic leukemia. Leuk Lymphoma 2013;54:1177–82.
47. Wan PT, Garnett MJ, Roe SM, Lee S, Niculescu-Duvaz D, Good VM, et al. Mechanism of activation of the RAF-ERK signaling pathway by oncogenic mutations of B-RAF. Cell 2004;116:855–67.
48. Jelinek DF, Tschumper RC, Stolovitzky GA, Iturria SJ, Tu Y, Lepre J, et al. Identification of a global gene expression signature of B-chronic lymphocytic leukemia. Mol Cancer Res 2003;1:346–61.
49. Sato H, Yazawa T, Suzuki T, Shimoyamada H, Okudela K, Ikeda M, et al. Growth regulation via insulin-like growth factor binding protein-4 and -2 in association with mutant K-ras in lung epithelia. Am J Pathol 2006;169:1550–66.
50. Wabakken T, Hauge H, Finne EF, Wiedlocha A, Aasheim H. Expression of human protein tyrosine phosphatase epsilon in leucocytes: a potential ERK pathway-regulating phosphatase. Scand J Immunol 2002;56:195–203.
51. Fujikawa K, Miletic AV, Alt FW, Faccio R, Brown T, Hoog J, et al. Vav1/2/3-null mice define an essential role for Vav family proteins in lymphocyte development and activation but a differential requirement in MAPK signaling in T and B cells. J Exp Med 2003;198:1595–608.
52. Vigorito E, Gambardella L, Colucci F, McAdam S, Turner M. Vav proteins regulate peripheral B-cell survival. Blood 2005;106:2391–8.
53. Burger M, Hartmann T, Krome M, Rawluk J, Tamamura H, Fujii N, et al. Small peptide inhibitors of the CXCR4 chemokine receptor (CD184) antagonize the activation, migration, and antiapoptotic responses of CXCL12 in chronic lymphocytic leukemia B cells. Blood 2005;106: 1824–30.

Published OnlineFirst March 8, 2016; DOI: 10.1158/1078-0432.CCR-15-2903

54. Messmer D, Fecteau JF, O'Hayre M, Bharati IS, Handel TM, Kipps TJ. Chronic lymphocytic leukemia cells receive RAF-dependent survival signals in response to CXCL12 that are sensitive to inhibition by sorafenib. Blood 2011;117:882–9.
55. Smal C, Lisart S, Maerevoet M, Ferrant A, Bontemps F, Van Den Neste E. Pharmacological inhibition of the MAPK/ERK pathway increases sensitivity to 2-chloro-2′-deoxyadenosine (CdA) in the B-cell leukemia cell line EHEB. Biochem Pharmacol 2007;73: 351–8.
56. Yusa K, Zhou L, Li MA, Bradley A, Craig NL. A hyperactive piggyBac transposase for mammalian applications. Proc Natl Acad Sci U S A 2011;108:1531–6.
57. Wang W, Lin C, Lu D, Ning Z, Cox T, Melvin D, et al. Chromosomal transposition of PiggyBac in mouse embryonic stem cells. Proc Natl Acad Sci U S A 2008;105:9290–5.
58. Scholl C, Frohling S, Dunn IF, Schinzel AC, Barbie DA, Kim SY, et al. Synthetic lethal interaction between oncogenic KRAS dependency and STK33 suppression in human cancer cells. Cell 2009;137:821–34.

Published OnlineFirst March 8, 2016; DOI: 10.1158/1078-0432.CCR-15-2903

Clinical Cancer Research

Transposon Mutagenesis Reveals Fludarabine Resistance Mechanisms in Chronic Lymphocytic Leukemia

Tatjana Pandzic, Jimmy Larsson, Liqun He, et al.

Clin Cancer Res 2016;22:6217-6227. Published OnlineFirst March 8, 2016.